TECHNOLOGICAL METHODS OF PREVENTING SLOPE ANGLE VIOLATIONS IN THE MINE. MEASURING SLOPE ANGLES.

Djaksimuratov Karamatdin Mustapaevich[1]
[1]Candidate of Natural Sciences, Nukus Mining Institute
Maulenov Nurlibek Axmet o'g'li[2]
[2]Student of Nukus Mining Institute:
Ametov Ruslan Muxtar o'g'li[3]
[3]Student of Nukus Mining Institute:
Joldasbayeva Aysulu Baxitbay qizi[4]
[4]Student of Nukus Mining Institute:
Embergenov Allabergen Polatbay o'g'li[5]
[5]Student of Nukus Mining Institute:
https://doi.org/10.5281/zenodo.7107279

Abstract: Slope failures are an inevitable aspect of economic pit slope designs in the mining industry. Large open pit guidelines and industry standards accept up to 30% of benches in open pits to collapse provided that they are controlled and that no personnel are at risk. Rigorous ground control measures including real time monitoring systems at TARP (trigger-action-response-plan) protocols are widely utilized to prevent personnel from being exposed to slope failure risks. Technology and computing capability are rapidly evolving. Aerial photogrammetry techniques using UAV (unmanned aerial vehicle) enable geotechnical engineers and engineering geologists to work faster and more safely by removing themselves from potential line-of-fire near unstable slopes. Slope stability modelling software using limit equilibrium (LE) and finite element (FE) methods in three dimensions (3D) is also becoming more accessible, user-friendly and faster to operate. These key components enable geotechnical engineers to undertake site investigations, develop geotechnical models and assess slope stability faster and in more detail with less exposure to fall of ground hazards in the field. This paper describes the rapid and robust process utilized at BHP Limited for appraising a slope failure at an iron ore mine site in the Pilbara region of Western Australia using a combination of UAV photogrammetry and 3D slope stability models in less than a shift (i.e. less than 12 h).

Keywords: Slope stability,3D limit equilibrium analysis,Aerial imagery, Photogrammetry,Open pit mining.

Introduction

In both civil engineering and mining projects, practical limitations significantly affect the ability to assess the stability of rock slope cuttings and benches in real-time, using analytical approaches such as kinematics, LE, FE or distinct element modelling. Excavation is usually too fast for this. Two key limitations currently preventing this are:

1. Time required for local site investigations. In the case where slope failures occur, safety concerns and residual risks in close proximity to unstable slopes such as failure reactivation or localized rock falls may prevent site investigations altogether;
2. Time required to translate the site investigation data into a geotechnical model to facilitate detailed stability analysis using a variety of numerical codes.

Traditional rock slope mapping techniques would typically require from 30 to 180 min of field time to assess a 10 m length of slope using window and traverse approaches, respectively.

Development or refinement of a geotechnical model and subsequent stability analyses can easily take several hours thereafter. In contrast, empirical methods such as slope mass rating (SMR), Q-slope and slope stability assessment methodology (SSAM) can be applied in real-time to assess stability as slopes are exposed in the field. Typically, these empirical methods require between 5 and 15 min in the field to assess slope stability for a 10 m long section. Slope stability modelling techniques have significantly improved over the years from basic kinematic analysis in the 1990s through to two-dimensional (2D) LE analysis and simple FE modelling using PC in the 2000s. However, in Australian iron ore and coal deposits, open pit mines are typically designed using relatively limited data density and the routine use of more advanced numerical modelling techniques such as FLAC and UDEC is generally not practicable, nor is it always warranted. indicated that over 80% and 90% of coal mines are designed using kinematics and 2D LE analysis, respectively, and that less than 15% of designs include 3D numerical analyses. The recent development and improvement of simple-to-use 3D LE and FE analysis software has provided an additional method for identifying potential issues in slope designs [11,12]. The use of 3D analysis has also been shown to provide more detailed analysis results that allow geotechnical engineers to optimize pit slope designs and unlock resource value.

Technological quality of iron ore deposits

The central and eastern Pilbara region of Western Australia is renowned for its abundance of economically extractable, bedded iron ore deposits between the townships of Newman and Port Hedland. BHP Limited currently operates over 50 individual open cut mines across six mining hubs: Whaleback, Eastern Ridge, Jimblebar, Yandi, Mining Area C and South Flank (Fig. 1). Due to the broad regional expanse of the operations, a very high extraction rate is achieved despite vertical development rates remaining relatively low (typically 1–3 benches or 10 to 30 m per year in an individual iron ore pit). Final pit depths generally range from less than 100 to 450 m. Iron ore deposits in the Pilbara region occur within banded iron formations of the Hamersley Group which comprises Archaean to Proterozoic marine sedimentary and volcanic rocks. Geological structures play a key role in the location, geometry and preservation of high grade iron ore bodies. The structural evolution of the Hamersley Province is considered to be well understood and is documented by Dalstra. In general terms, it comprises normal faulting and thick-skinned tectonics in the west and more intense folding, minor thrust faulting and possible thin-skinned tectonics on the east. Some deposits such as Whaleback are very complex with several phases of deformation, resulting in an overturned stratigraphic sequence. The stratigraphic units of economic interest consist of banded iron formation (BIF) with interbedded carbonates and shales. BIF can vary in thickness due to differing amounts of carbonate dissolution and silica replacement during iron ore enrichment formation and typically contain thick interbedded shale bands, some of which make excellent stratigraphic marker horizons in the mining areas as they are remarkably persistent across hundreds of kilometers throughout the Hamersley Province. The bedded iron ore deposits are hosted in highly anisotropic rock masses. Anisotropy, as defined in engineering geology, refers to a rock whose engineering properties (such as strength and permeability) vary with direction. Anisotropy is very common and present everywhere. Isotropy is rare. Anisotropy is produced as a consequence of the geological history of the rock or rock mass, and generally has its origins in the varying mineralogical composition of different layers and/or a preferred orientation of mineral grains. Distinctive bedding planes are produced in sedimentary rocks

due to depositional cycles as is the case in iron ore. Two distinct scales of anisotropy are prevalent (Fig. 2): (1) bedding scale–between individual bedding planes (e.g. BIF-BIF or shaleshale bedding planes), and (2) banding scale–between known specific bands within stratigraphic layers (e.g. shale band NS2 and the bands of BIF either side in the Newman Member). Planar sliding along adversely oriented and low strength shale bands is the most common mode of slope instability from bench to overall slope scale in mining operations and also within natural slopes of the Pilbara region. The slope failure from the BHP mine discussed in this paper is a classic example of multi-bench planar sliding in the Hamersley Group (Fig. 3). The failure itself was ‘‘controlled” by means of a catchment bund such that no personnel or equipment were exposed to the hazard as shown in Figs. 4 and 6–8. Rock mass and bedding shear strengths are typically well understood in the Pilbara region as relatively limited variation exists across individual deposits that are situated within the same stratigraphic unit. Intact rock and rock mass shear strength, particularly in BIF-dominated stratigraphic units, may vary quite significantly with weathering, and to a lesser extent, alteration.

There is no significant difference between the shear strength of bedding planes of shale and BIF units across the Pilbara. The shear strength of shale bedding planes is also generally independent of weathering grade. Failure back-analyses, site

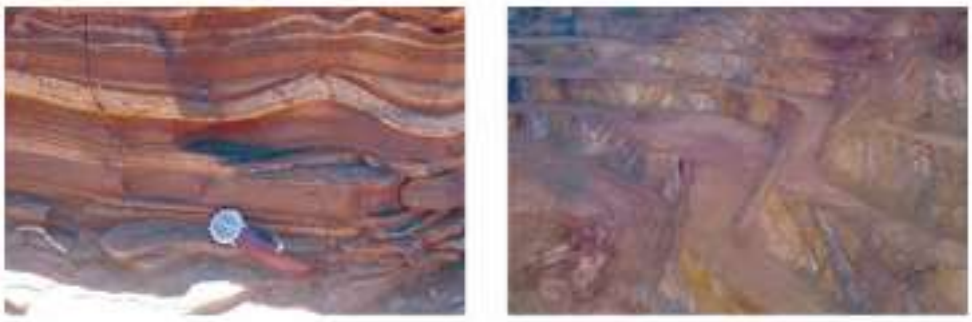

(a) Bedding scale

(b) Banding scale in an iron ore pit with 12 m high benches

Fig. 2. Scales of anisotropy in Western Australian iron ore deposits

Fig. 3. Aerial reconnaissance of planar sliding failure mechanism at BHP mine.

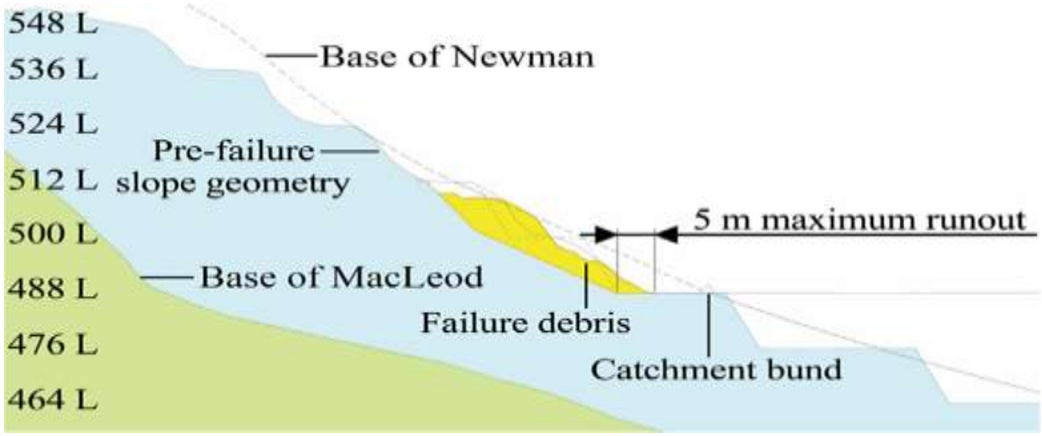

Fig. 4. Geological cross-section through failure.

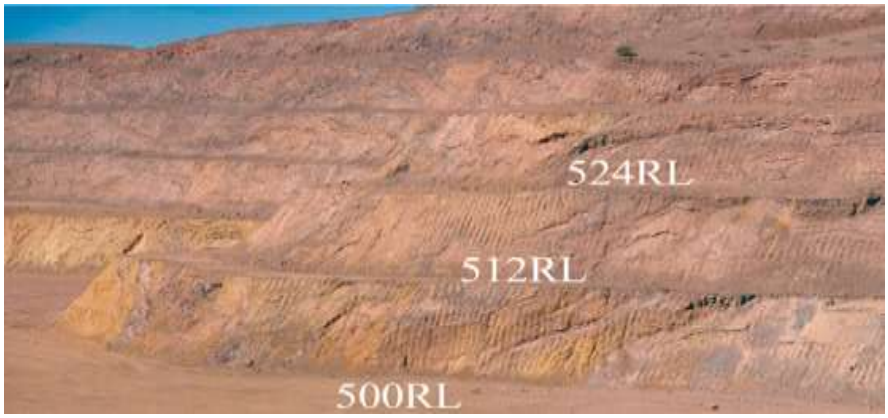

Fig. 5. Pit slope with undercut bedding planes near convex slope profile in July 2019–pit floor 500 RL

Fig. 6. Pit slope with initial 8 m high failure contained within a rock fall catchment bund on 26 October 2019–pit floor 492 RL

Fig. 7. Pit slope failure propagation to 15 m high contained within a larger failure catchment bund on 26 November 2019–pit floor 488 RL.

Fig. 8. South wall failure propagation to 24 m high on 27 November 2019–pit floor 488 RL

specific drilling and laboratory testing provide a means of assessing variation in shear strengths and material density. Slope stability analyses are undertaken considering the effects of anisotropy: (1) bedding scale anisotropy can and should be modelled using directional shear strength models in 2D or 3D; and (2) banding scale anisotropy is best modelled using discrete weak bands in both 2D and 3D models rather than with directional shear strength models. The use of directional shear strength models for banding scale anisotropy allows the weakness plane to appear ubiquitously in this slope, rather than at its actual discrete location. This may result in over-conservatism. Seery conceptually compared using ubiquitous directional shear strength models against discretely located shale bands within the Dales Gorge Member of the Brockman Iron Formation. Seery concluded that the directional shear strength model does not necessarily honor the geology, particularly due to the widely spaced shale bands in the Dales Gorge Member. In order to achieve an optimal slope design, it is necessary to understand the geology, and have the ability to discretely model banding scale anisotropy (i.e. discretely model shale bands) coincidentally with bedding scale anisotropy. Notwithstanding this, it remains appropriate to use a ubiquitous shale band strength model however where the position of discrete shale bands is not known. As slopes become exposed with mining progression, a detailed reconciliation process is used to validate the location of shale bands and enable a transition from a ubiquitous shale band strength model to discretely modelling banding scale anisotropy.

Aerial reconnaissance and photographic records

Aerial reconnaissance using UAV is routinely used to inspect unstable or failed slopes in both civil and mining engineering applications. High resolution imagery and video are captured while ensuring the geotechnical engineer or surveyor remains at a safe distance, away from the line-of-fire of potential rock falls or further instability. Fig. 3 provides examples of aerial reconnaissance imagery from the planar sliding failure at the BHP iron ore mine. Failure geometry and geological conditions are illustrated in Fig. 4, and ultimately comprised: (1) failure height of 24 m, (2) failure width of 40 m, (3) maximum horizontal runout of 5 m on pit floor (contained within catchment bund), and (4) estimated failure size of 15000 tons. The planar failure mechanism was progressive, initiating as a local bench failure that propagated further with the progression of mining excavations and increased loading of the undercut shale band. Fig. 5 shows the pit slope prior to the failure with the pit floor 500 RL in July 2019. Bedding planes near the convex slope profile are undercut and some shale bands exposed.

Also visible are several areas of local bench crest losses. Excavations progressed vertically downward 8 m (pit floor 492RL), undercutting a pervasive shale band and initiating a bench failure as shown in Fig. 6. Further excavation, vertically downward 4 m (pit floor 488 RL) was successful in extracting ore and achieving the planned pit design; however, further deterioration of the initial bench failure was observed. Failure propagation was evident on 26 November 2019 as shown in Fig. 7. The rate of failure may have been exacerbated by 0.8 mm of rainfall that occurred on 27 November 2019, resulting in the 24 m high failure shown in Fig. 8.

UAV photogrammetry and geotechnical model update

Photogrammetry enables the generation of 3D models from a series of overlapping photographs. The introduction of the ‘‘structure from motion” concept as well the broad availability of drones or UAV brought a renaissance of this technology. Structure from motion includes a series of processing steps that allows computing a comprehensive set of 3D surface points that are combined to a surface description (i.e. a mesh) in photo-realistic style. Due to the availability of redundant information, geometric deviations present in camera used (i.e. lens distortion) are compensated while generating the 3D model. This auto-calibration ability makes modern photogrammetry algorithms capable of producing accurate 3D models even from low-grade cameras, so even low cost, off-theshelf drones can be used to generate 3D models at sufficient high accuracy. Several commercial software packages are available for modern photogrammetry (e.g. Agisoft, Pix4D, ShapeMetriX). All work in a similar way and provide comparable results. In this case study, ShapeMetriX software has been used since it also includes tools for geological and geotechnical mapping. Figs. 9 and 10 show the resultant 3D model generated from 284 photographs captured using a 9 mm digital camera mounted on a DJI Phantom 4 drone. The model computed in less than one hour on a mobile workstation (2017 Alienware 17 R4). It consists of over 7 million surface points and has a ground sample distance (GSD) of 2 cm per pixel. Note the lighter material on the right hand side of the model in Fig. 10; this is where bench failures and crest losses had previously occurred on daylighting shale bands. Model accuracy in that context needs to be looked at in at least two ways: (1) positional accuracy, i.e. the correct location of the 3D model and given coordinate grid or the correct orientation and scale of the model if working in local co-ordinates, and (2) shape accuracy that reflects mainly if all the details of the rough surface are rendered by the 3D model. It is linked with the GSD and spacing of the 3D surface points. Positional accuracy is best if there are some reference points (ground control points or GCP) in the captured area. The GCPs are locations with surveyed coordinates. The referencing mechanism transforms the model to the location of the GCPs with remaining residuals in the sub-centimeter range. In some cases, the installation and surveying of GCPs is timeconsuming and costly especially in regions that are difficult to access such as alpine rock fall areas. Similarly, in an active mining area where personnel can be exposed to interaction with haul trucks and other mining equipment, GCPs may not be practicable from a safety perspective. In such case, the 3D model may be referenced (scaled and oriented) based only on GPS information recorded while taking the images. Such models show larger deviations from the ground truth–depending on the quality of GPS (the absolute localization might be some meters off). However, when comparing an accurately geo-localized 3D model using GCP and a roughly localized model using GPS, the scale and orientation of the 3D models align within 1% (i.e. shape accuracy is unaffected). Such pure GPS referencing can be even improved by using real time kinematic

(RTK) or post processed kinematic (PPK). Both lead to better absolute geo-localization of the 3D model without GCPs. 3D models developed from pure GPS referencing showed to be sufficiently scaled and oriented for performing geological mapping. In particular, data such as discontinuity orientations or spacing are practically unaffected since variations or errors in the 3D model (from UAV photogrammetry) are more than an order of magnitude less than errors obtained when using conventional measuring techniques such as mapping using a geological compass, tape measure or orienting and logging discontinuity orientations in drill core. ShapeMetriX software allows direct analysis of geometric entities such as volumes, areas, distances, sections, and the measurement of point coordinates. In addition, geologically relevant features can be examined. By way of example, Fig. 11 illustrates orientations of traces and surfaces that can be interpreted. Recent developments provide automatic analyses which lead to reproducible and statistically admissible assessments due to the high number of individual measurements.

Fig. 10. 3D model developed from UAV photogrammetry with the planar failure on the left hand side near the convex slope profile. Lighter colored material on the right hand side where repetitive bench crest losses have occurred shows near-planar shale bedding planes. Shape accuracy is <5 cm without GCP.

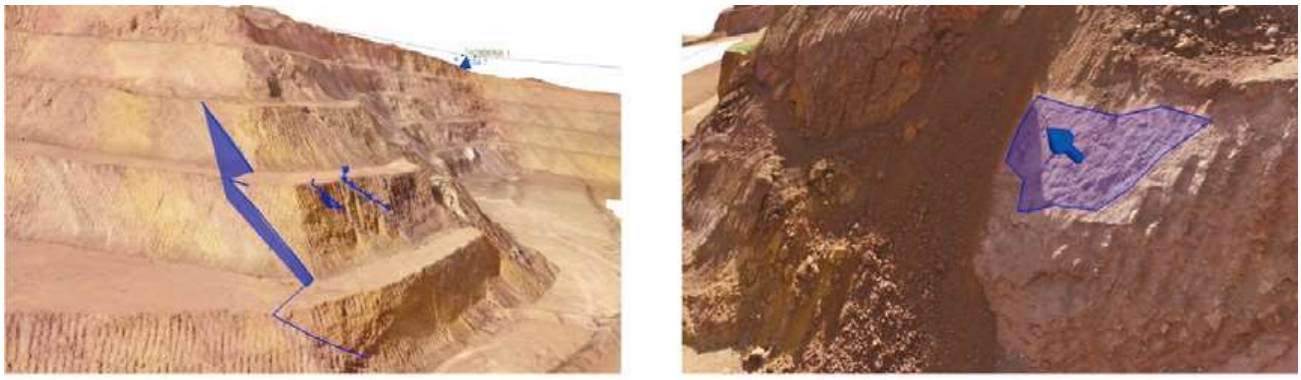

(a) Orientation of significant shale bedding plane traces

(b) Shale bedding surface trace

Fig. 11. Orientation measurement of significant shale bedding plane traces across multiple benches and shale bedding surface trace upon which planar sliding has already occurred.

A total of 198 geological structures including bedding planes and joints were mapped using ShapeMetriX (Fig. 12) and imported into a 3D CAD package (GEM4D) where the failure plane was modelled as a 3D surface. The failure plane was a distinct shale band that was located near the MacLeod-Newman geological contact. The orientation, or rather, the dip of this shale

band was approximately 3———————————-5——————————— shallower than predicted in the pre-mining geological model, resulting in undercutting near the base of the slope (i.e. the pre-mining geological model was highly reliable).

Slope stability analysis

2D and 3D limit equilibrium modelling

Slope stability analyses can be undertaken in 2D or 3D. Traditionally, 2D models were generally most commonly constructed due to the relative ease of model construction and rapid computation time compared to 3D models. 2D models will generally yield a conservative result where: (1) the shear resistance of the end surfaces of failures is not included in the modelling process, and (2) cross-sections selected for FoS (factor of safety) calculation are typically a worst-case scenario which will generally not be representative of all slope conditions. However, this is not always the case, where 3D analysis can also produce lower FoS than 2D analysis. Wines stated that the main reason for the differences in results between 2D and 3D analysis is the ability of 3D analysis to provide an accurate

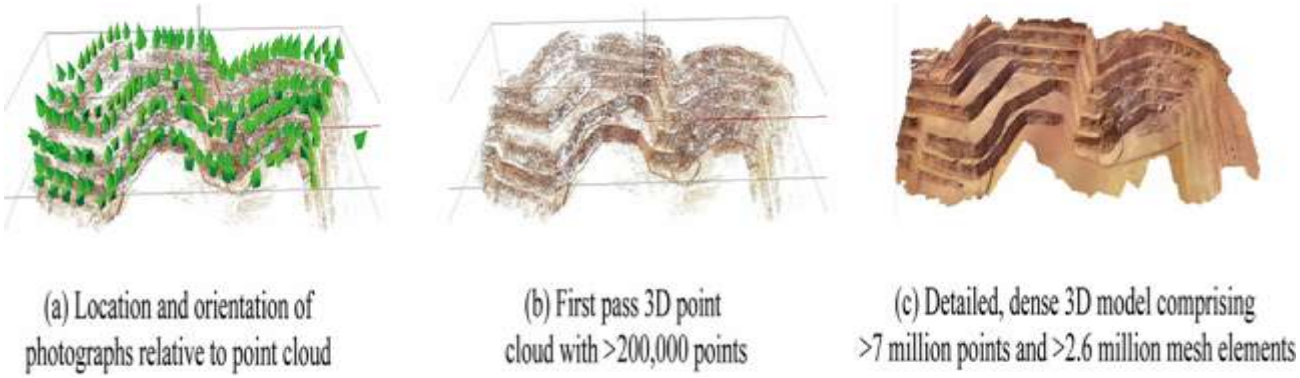

(a) Location and orientation of photographs relative to point cloud

(b) First pass 3D point cloud with >200,000 points

(c) Detailed, dense 3D model comprising >7 million points and >2.6 million mesh elements

Fig. 9. 3D model developed from UAV photogrammetry covering surface area of approximately 186000 m^2.

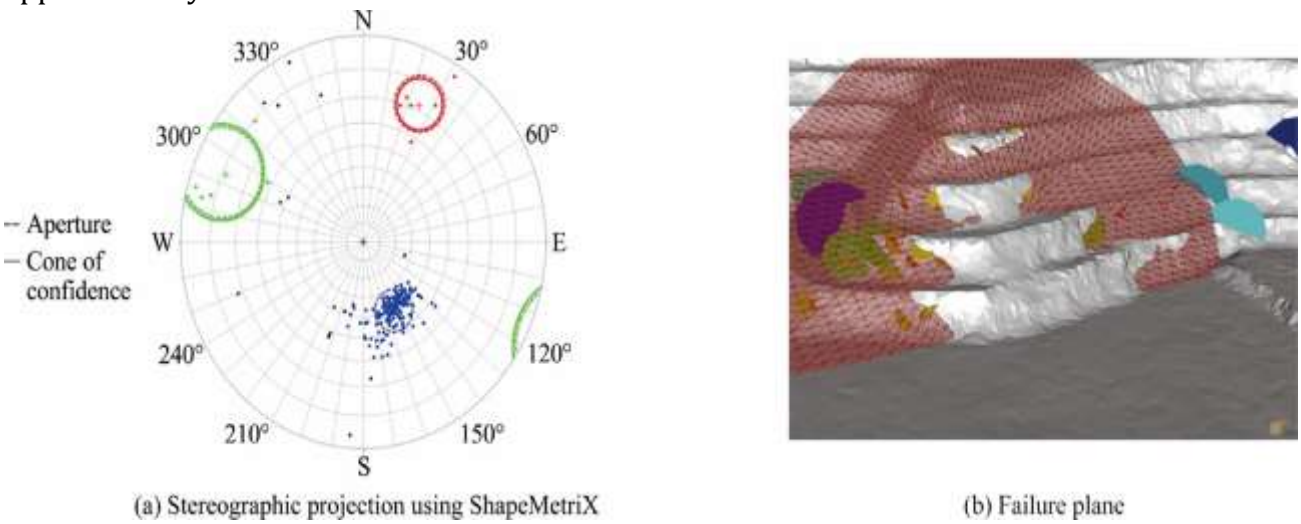

(a) Stereographic projection using ShapeMetriX

(b) Failure plane

Fig. 12. Stereographic projection showing bedding planes: 40———————————/333 (blue) and joints: 72———————————/205——————————— (red) and 79———————————/113——————————— (lime) in ShapeMetriX and planar sliding failure plane (shale band) re-evaluated in GEM4D to create a wireframe mesh from utilizing the imported geological structures which are represented as colored disks. (For interpretation of the references to colour in this figure legend, the reader is referred to the web version of this article.) representation of the problem such as geometry, spatial

distribution of geotechnical domains, discontinuity orientations and distribution of pore pressures, all which will always are threedimensional in reality. Wines and Sjoberg stated that for relatively long open pits with basic geological conditions a 2D model can generally be justified, except at the pit corners and at the lateral bounds of slope failures. Lorig & Varona recommend 3D assessments of slope stability should be made where the strike of discontinuities is less than 20———————————— to 30———————————— from the strike of the excavated face. Bar & Weekes demonstrated that anisotropy (or true dip) of any structure can only be correctly modelled in 3D as 2D sections of a slope inherently result in an apparent dip which is not completely perpendicular to the anisotropy. Bar & McQuillan presented several case studies from open pit iron ore and coal mines that highlight the limitation of 2D LE models in highly anisotropic geological settings. The case studies presented show 2D LE analysis can lead to either the over-estimation or under-estimation of FoS where 2D analysis did not adequately model the anisotropic conditions under which failure occurred. Stated that to reliably predict the performance (e.g. propensity for failure) and critical failure mechanism (including spatial location) of slope failure, geotechnical engineers must select appropriate tools to complete slope stability assessments. Modelling techniques which can adequately account for the failure mechanisms typically observed in highly anisotropic geological settings, such as WAIO iron ore deposits, include empirical, 3D LE and 3D numerical (e.g. FE) modelling. Of these three methods, LE has become a preferred method for routine slope stability analysis since its introduction in the early 20th century. Its popularity stems from its ease of use, relatively fast calculation speed and calibration from years of application and observation. A FoS using LE methods can be calculated using the method of slices (2D analysis) or method of columns (3D analysis). Both methods are based on the principle of statics, where the summation of forces acting on a failure surface (i.e. mobilized stress) are compared with the sum of the forces available to resist failure (i.e. available shear resistance). The ratio between these two sums is defined as the FoS. If the FoS is greater than 1, the slope is assumed to be stable. Geotechnical engineers frequently set design acceptance criteria (DAC) at values much higher than FoS = 1 when determining a stable slope design. That is, FoS of 1.2, 1.3, 1.5, etc., are required for varying slope configurations with varying required serviceability and strategic risk. complex surface, is discretized into vertical columns as shown in Fig. 13. Forces are analogous to the vertical slice method used in 2D. In 3D, each column has a share cross-section and forces and moments are solved in two orthogonal directions. Vertical forces determine the normal and shear force acting on the base of each column.

Pre-mining geotechnical design

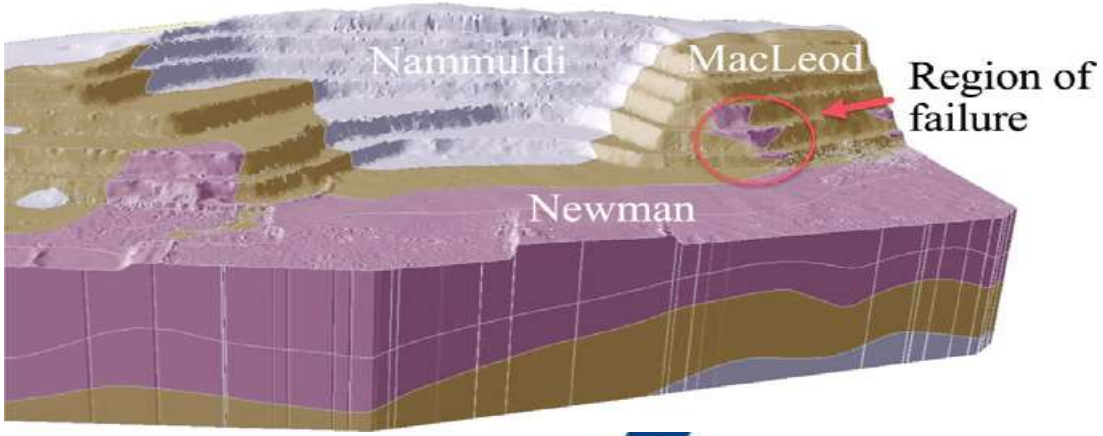

Updated geotechnical model for south wall represented in 3D for LE analysis using Slide3.

Member, which also appears locally within the slope in areas where both slope and stratigraphical geometries permit, including the region of failure. The current pit is significantly above the groundwater table, so dry conditions are appropriate for the slopes. presents the original geotechnical design shear strength parameters derived from diamond core drilling and laboratory testing using Hoek-Brown failure criterion for rock mass, 2D LE analysis was used to design the pit slopes to meet the DAC whereby the FoS 1.2 for inter-ramp and overall slopes. The original (pre-mining) geotechnical design for the pit identified single to multiple bench scale hazards on the south wall using a combination of 2D LE and kinematic analyses from which the probability of undercutting bedding planes was expected to be in the order of 50%. As such, the area was routinely inspected and included as part of the slope validation process whereby actual ground conditions are reconciled against original geotechnical design predictions. During the course of mining five benches (i.e. vertically downward 60 m), several local single bench failures ——————————— 12 m in height had occurred, either during blasting, or excavation. These were safely remediated with standard mining procedures. Using the 3D model developed from UAV photogrammetry, Fig. 15 reconciles the actual percentage of slope face area that had been involved with failure events. The failure areas represent 32% of the total slope area (i.e. slope performance was better than expected since this is significantly less than the predicted 50% from probability of undercutting assessments).

3D limit equilibrium back-analysis of failure

The 24 m high planar failure in Fig. 3 was back-analyzed to refine the original geotechnical design shear strength parameters to enable add rigor to the geotechnical model and enable better prediction of future ground behavior as mining continues. The 3D LE model was developed such that it is spatially large enough to enable subsequent re-evaluation of future pit slope stability and alternative designs, if required. The updated geotechnical model including the location and orientation of the failure plane (shale bedding) and updated stratigraphic wireframes derived from UAV photogrammetry were utilized in the 3D LE back-analysis.

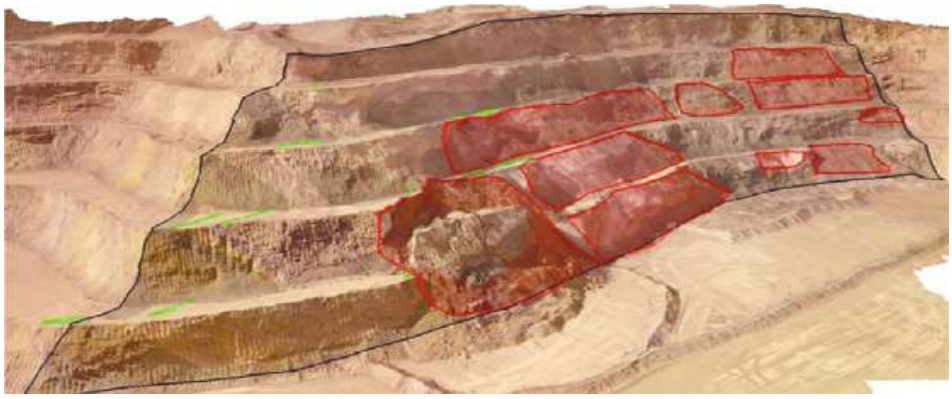

Fig. 15. UAV photogrammetry 3D model illustrating failure event areas in red, total failure area in black, and visible tension crack traces in lime green using ShapeMetriX. (For interpretation of the references to colour in this figure legend, the reader is referred to the web version of this article.)

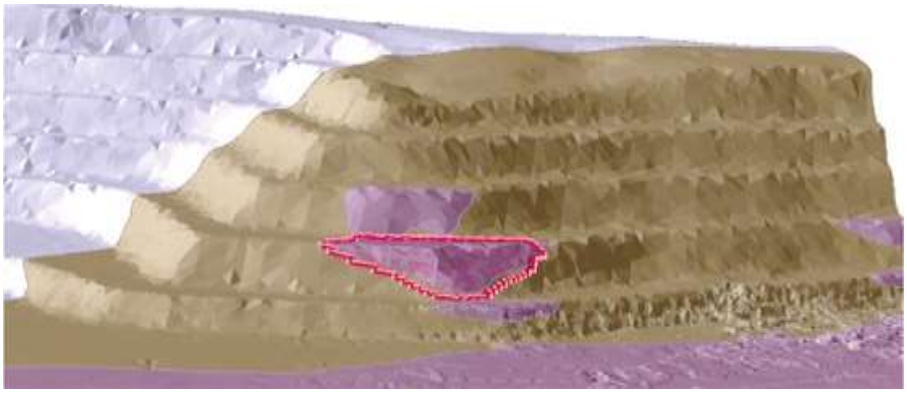

Fig. 16. Planar sliding failure back-analysis using bedding shear strength parameters, c'=0 kPa and /'=29———————————, identifying initial single bench instability.

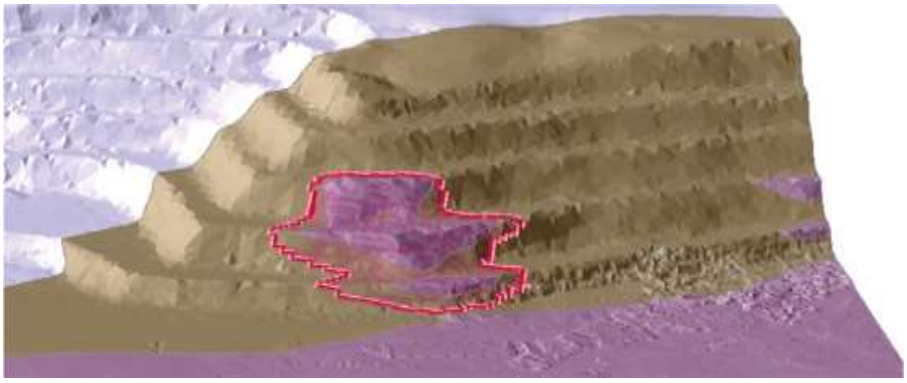

Fig. 17. Planar sliding failure back-analysis using bedding shear strength parameters, c'=5 kPa and /'=26———————————, identifying larger mechanism.

The 3D LE back-analyses results indicated bedding shear strengths likely contained 0 to 5 kPa of cohesion with friction angles ranging from 26——————————— to 29———————. Vibration and gas pressures from blasting along the already weaker shale bedding planes likely resulted in a loss of, or at least, significant degradation of cohesion, that initiated the planar failure. The future pit slope design was re-evaluated based on the bedding shear strengths obtained from the back-analysis as well as updated stratigraphical wireframes derived from the UAV photogrammetry.

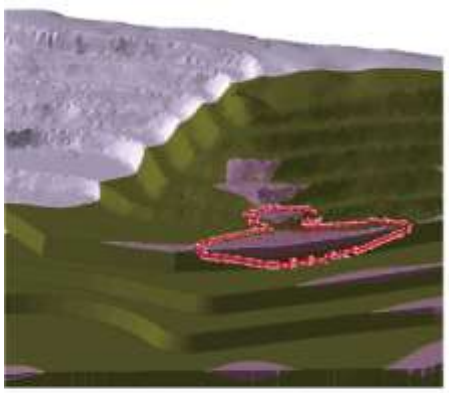

(a) FoS=1.09 for single 12 m high bench

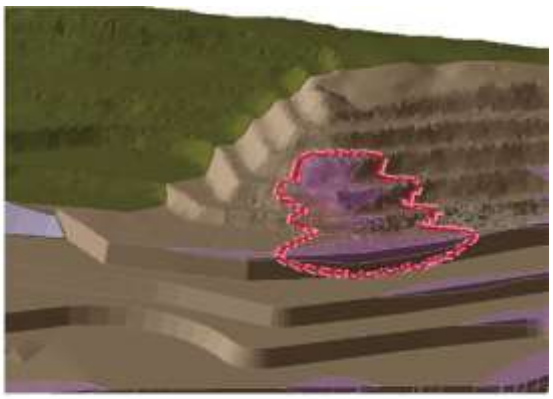

(b) FoS=1.20 for 48 m high multiple bench slope

Fig. 18 illustrates key findings of the 3D LE analysis results of the future pit slope:

(1) FoS = 1.09 for a single bench failure mechanism was identified (Fig. 18a). Although not complying with the design acceptance criteria, associated risks of a potential failure can be managed through the wide catchment berm as well as slope deformation monitoring.

(2) FoS = 1.20 for a 48 m high multiple bench slope was identified and complied with the DAC (Fig. 18b). Notwithstanding this, slope validation will routinely continue with mine progression to ensure that if any significant deviations to the geotechnical model are observed, they can be acted upon.

No evidence of larger slope failure risks using the updated geotechnical model.

Discussion

Aerial reconnaissance, photogrammetry, and 3D LE modeling were used to rapidly appraise ground conditions and stability conditions for the current and future planned slopes at the BHP iron ore mine. Demonstrates that through the use of the latest tools and technology, the process can be successfully completed in less than 12 h. The ability to respond quickly to geotechnical events enables the geotechnical team to provide quality advice to mine operation to continue operating safely and economically.

The ease and speed of undertaking UAV photogrammetry make it a powerful tool for identifying the location, orientation and length of geological structures. However, it should be noted that photogrammetry application on its own remains limited in its capability of undertaking complete ground characterization. By way of example, joint properties such as infilling and intact rock parameters such as strength cannot be evaluated or estimated using this method and required physical time spent in the field where safely accessible. The BHP WAIO survey team uses UAV photogrammetry for routine end-of-month surveying. With the addition of minor extra flights to capture additional angles and higher resolution digital SLR camera photographs, the geotechnical engineering and geology teams are also enabled to routinely update geotechnical and structural geological models across operating pits. Future improvements to the process include the use of high-precision UAV that remove the need for ground control points while maintaining or improving aerial reconnaissance and photogrammetry accuracy.

Conclusion

Since mid-2019, the BHP WAIO geotechnical engineering team has routinely been analyzing pit slope stability using 3D LE software Slide3. The shift to 3D modelling from 2D cross-sections has facilitated better integration with mine planning and is increasing the speed (and quality) at which we can review proposed pit slope designs. Quite simply, new mine and pit slope designs are inserted into a 3D model, replacing their predecessor. This approach also has the ability to automatically generate and analyze 2D cross-sections that are directly comparable with historic analyses. The 3D models themselves provide significant insight into possible lateral extents of failure mechanisms such that sensible advice can be provided to mine operations in terms of geotechnical risk management without the need for overly conservative slope designs.

References:

1.Joass GG, Dixon R, Sikma T, Wessels SDN, Lapwood J, de Graaf PJH. Risk management and remediation of the north wall slip, West Angelas Mine, Western Australia. In: Proceedings of international symposium on rock slope stability in open pit mining and civil engineering – slope stability 2013. Brisbane; 2013. p. 1–16.

2. Lucas DL, de Graaf PJH. Iterative geotechnical pit slope design in a structurally complex setting: a case study from Tom Price, Western Australia. In: Proceedings of

international symposium on rock slope stability in open pit mining and civil engineering – slope stability 2013. Brisbane; 2013. p. 513–26.
3. Seery JM. Limit equilibrium analysis of a planar sliding example in the Pilbara Region of Western Australia – comparison of modelling discrete structure to three anisotropic shear strength models. In: Proceedings of SAIMM slope stability 2015. Cape Town; 2015. p. 681–96.
4.Maldonado A, Haile A. Application of ANOVA and Tuckey-Cramer statistical analysis to determine similarity of rock mass strength properties across Banded Iron Formations of the Pilbara region in Western Australia. In: Proceedings of SAIMM slope stability 2015. Cape Town; 2015. p. 15–33.
5.Maldonado A, Mercer KG. Comparison of the laboratory and Barton-Bandis derived shear strength of bedding partings in fresh shales of the Pilbara, Western Australia. In: Proceedings of ISRM international symposium - ARMS10. Singapore; 2018.
6. Maldonado A, Mercer KG. An investigation into the shear strength of bedding planes in shale materials from the Hamersley Group rocks in the Pilbara region of Western Australia. In: Proceedings of SAIMM slope stability 2015. Cape Town; 2015. p. 47–62.
7.Saroglou C, Kallimogiannis V, Bar N, Manousakis G, Zekkos D. Analysis of slope instabilities in the Corinth Canal using UAV-enabled mapping. In: Proceedings of ICONHIC 2019, 2nd international conference on natural hazards & infrastructure. Chania; 2019.
8. Snavely N, Seitz SM, Szeliski R. Modeling the world from internet photo collections. Int J Comput Vision 2008;80(2):189–210.
9.Buyer A, Pischinger G, Schubert W. Image-based discontinuity identification. Geomech Tunnelling 2018;11(6):693–700.
10.Gaich A, Pötsch M, Schubert W. Digital rock mass characterization 2017 – Where are we now? What comes next? Geomech Tunnelling 2017;10 (5):561–6.